Equatorial noise emissions with a quasi-periodic modulation observed by DEMETER at harmonics of the O+ ion gyrofrequency

Michel Parrot, František Němec, Ondřej Santolík, Nicole Cornilleau-Wehrlin

AGU PUBLICATIONS

JGR

Journal of Geophysical Research: Space Physics

RESEARCH ARTICLE
10.1002/2016JA022989

Key Points:
- Equatorial noise with QP emissions observed in the ionosphere
- They are observed during the recovery phase of intense magnetic storms
- They are observed at harmonics of the O^+ ion gyrofrequency

Correspondence to:
M. Parrot,
mparrot@cnrs-orleans.fr

Citation:
Parrot, M., F. Němec, O. Santolík, and N. Cornilleau-Wehrlin (2016), Equatorial noise emissions with a quasiperiodic modulation observed by DEMETER at harmonics of the O^+ ion gyrofrequency, *J. Geophys. Res. Space Physics*, *121*, doi:10.1002/2016JA022989.

Received 23 MAY 2016
Accepted 22 SEP 2016
Accepted article online 23 SEP 2016

Equatorial noise emissions with a quasiperiodic modulation observed by DEMETER at harmonics of the O^+ ion gyrofrequency

Michel Parrot[1], František Němec[2], Ondřej Santolík[2,3], and Nicole Cornilleau-Wehrlin[4,5]

[1]LPC2E/CNRS, Orléans, France, [2]Faculty of Mathematics and Physics, Charles University in Prague, Prague, Czech Republic, [3]Institute of Atmospheric Physics, Czech Academy of Sciences, Prague, Czech Republic, [4]Laboratoire de Physique des Plasmas, Ecole Polytechnique, CNRS, Palaiseau, France, [5]LESIA, Observatoire de Meudon, Meudon, France

Abstract The analysis of ionospheric equatorial noise (EN) with a quasiperiodic (QP) modulation observed by the Detection of Electro-Magnetic Emissions Transmitted from Earthquake Regions (DEMETER) spacecraft is presented. These EN emissions, also called whistler mode or fast magnetosonic waves, play an important role in acceleration of radiation belt electrons. A statistical analysis with 103 events shows that they occur just after intense magnetic storms. Usually, they are generated by unstable proton ring distribution close to the magnetic equator at harmonics of the proton gyrofrequency in the inner magnetosphere ($2 < L < 8$). But at lower L values down in the ionosphere three events have been analyzed and it appears that the EN waves are at harmonics of—or very close to—a O^+ ion gyrofrequency which can be found close to or slightly above the satellite. The wave propagation analysis indicates that these emissions are coming from an area above the satellite. Concerning one event, the EN emissions are observed on several consecutive orbits and there is a temporal coincidence with observations performed by the Cluster satellites at higher altitudes in the magnetosphere. EN emissions at lower frequencies have been also observed by the Cluster satellites in the same longitudinal sector as DEMETER but at ~5 R_E. The analysis of the Spatio Temporal Analysis of Field Fluctuations data on board C1 reveals that the magnetic field spectrogram has peaks close to harmonics of the local proton gyrofrequency as usually reported. It is shown that the DEMETER and Cluster EN waves have a similar QP modulation but with slightly different period and frequency.

1. Introduction

Equatorial noise (EN) emissions, also referred to as whistler mode or fast magnetosonic waves, have been widely studied in the past [*Russell et al*., 1970; *Gurnett*, 1976; *Perraut et al*., 1982; *Kasahara et al*., 1994; *Santolík et al*., 2002; *Tsurutani et al*., 2014; *Posch et al*., 2015]. EN emissions are electromagnetic waves at frequencies between the proton cyclotron frequency and the lower hybrid resonance frequency, observed in the equatorial region. They appear as a series of narrow tones spaced at harmonics of the proton gyrofrequency in the source region [*Gurnett*, 1976; *Santolík et al*., 2002, 2004], and they propagate nearly perpendicular to the ambient magnetic field [*Chen and Thorne*, 2012], although the studies by *Boardsen et al*. [1992, 2016] placed estimates on the spread of the wave normal angles from the perpendicular direction.

About their generation mechanism, *Perraut et al*. [1982] using GEOS data noticed that these emissions are associated to a ring-like distribution of energetic protons. They presented a model to explain the main characteristics of these waves. *Horne et al*. [2000] confirmed the initial suggestion of *Gurnett* [1976] that these waves were generated by a cyclotron resonant interaction with injected ring current of energetic protons having ring distributions [see *Chen et al*., 2010, 2011; *Ma et al*., 2014]. It has been suggested that EN waves contribute to an energy transfer from the ring current to the Van Allen radiation belts [*Horne et al*., 2007; *Bortnik and Thorne*, 2010]. CRRES data have been used by *Meredith et al*. [2008] to confirm the association between EN waves and the presence of ion rings. *Balikhin et al*. [2015], using Cluster data, reported also an event where multiples of the proton gyrofrequency (from 17th up to 30th) have been observed simultaneously with a ring distribution of protons [see *Walker et al*., 2015a]. They obtained a good agreement between the calculated wave growth and their observation.

Recently, *Hrbáčková et al*. [2015] and *Němec et al*. [2015a] have done a systematic analysis of more than 2000 EN emissions recorded on board the four Cluster spacecraft between January 2001 and December 2010. They have shown that EN emissions are enhanced during disturbed periods and that they mostly occur between

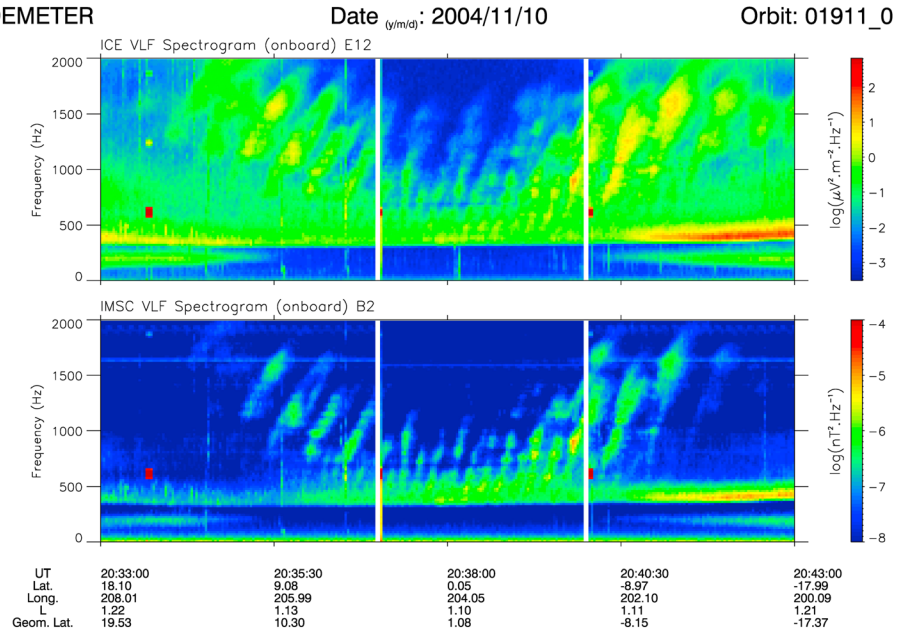

Figure 1. Spectrograms of (top) one electric component and (bottom) one magnetic component up to 2 kHz recorded on 10 November 2004 between 20:33:00 UT and 20:43:00 UT. The intensities of the spectrograms are color coded according to the scales on the right. The red spots at 625 Hz are due to internal calibration. The two vertical white lines delimit the time period when the wave experiment is in burst mode (i.e., between 20:37:00 and 20:40:00 UT). The parameters displayed below are the time in UT, the geographic latitude and longitude, the *L* value, and the geomagnetic latitude.

$L = 3$ and $L = 5.5$ within 7° of the geomagnetic equator. The emissions have higher frequencies and are more intense in the plasma trough than in the plasmasphere. They have estimated the spatiotemporal variability of the same events observed by several Cluster spacecraft. As a quasiperiodic (QP) time modulation of the wave intensity is present in more than 5% of the Cluster events, a study by *Němec et al*. [2015b] has shown that these EN events have a QP modulation with a period which is usually between 1 and 2 min (the overall spread is between 30 s and 4 min). They also noticed that the events occur during periods of increased geomagnetic activity and enhanced solar wind flow speeds.

Concerning the QP emissions, *Němec et al*. [2013a] have investigated their wave propagation parameters during a simultaneous event recorded both by Cluster and Detection of Electro-Magnetic Emissions Transmitted from Earthquake Regions (DEMETER). A more complete report of QP emissions observed by Cluster has been done by *Němec et al*. [2013b], and QP emissions in the ELF and VLF band observed by DEMETER have been systematically studied by *Hayosh et al*. [2014, 2016]. Their occurrence (mainly daytime after periods of enhanced geomagnetic activity), their frequency (from 500 Hz to 8 kHz), their time modulation (20 s in average), and their shape (mostly rising elements) have been investigated in *Hayosh et al*. [2014], whereas their propagation characteristics have been analyzed in *Hayosh et al*. [2016]. They have shown that the QP emissions propagate nearly perpendicular to the Earth's magnetic field B_0 at high latitudes, more oblique at midlatitudes, and even perpendicular to B_0 in the equatorial region. They claimed that this propagation pattern is consistent with a source of emissions located close to the equator at large radial distances. The periodic rising frequencies of the waves observed by *Fu et al*. [2014] and *Boardsen et al*. [2014] with the two Van Allen probes could be related to QP modulations. These QP modulations where simultaneously observed when VAP-B was deep inside the plasmasphere and VAP-A was outside [*Boardsen et al*., 2014]. This current paper will focus on EN with QP modulations and will show that they are propagating nearly perpendicular to the geomagnetic field down to altitudes as low as 700 km.

In the past, *Němec et al*. [2007] have underlined the difference between line structures of the EN emissions and the Magnetospheric Line Radiation which is observed at higher latitudes. Recently, *Santolík et al*. [2016] have studied an example of EN emissions without QP modulation observed by the low-altitude DEMETER satellite in the equatorial region and shown that the observed wave mode is decoupled from the low-frequency magnetosonic mode. This paper is devoted to the analysis of all EN emissions with QP

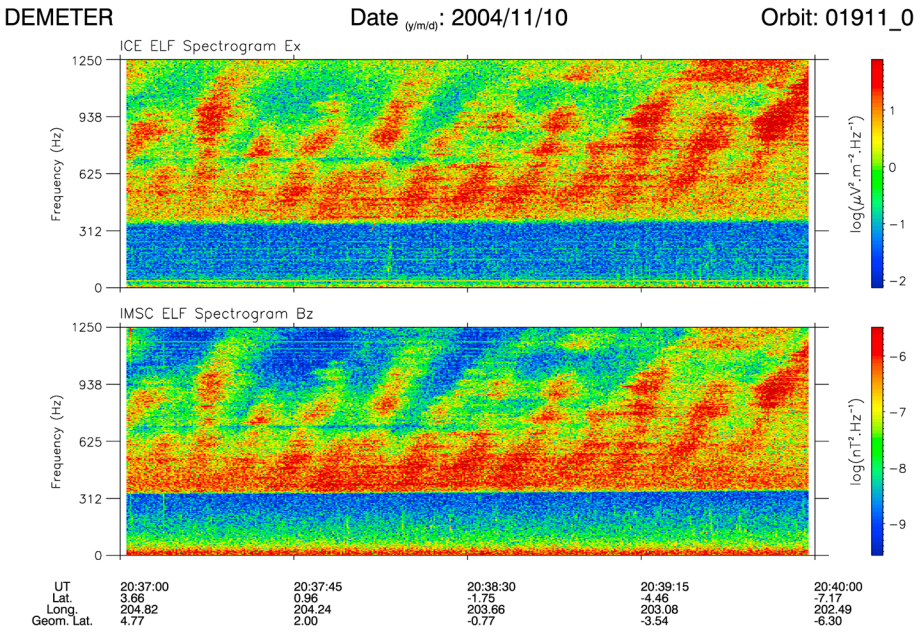

Figure 2. Zoom of Figure 1. Spectrograms of (top) one electric component and (bottom) one magnetic component up to 1.25 kHz recorded on 10 November 2004 between 20:37:00 UT and 20:40:00 UT. The intensities of the spectrograms are color coded according to the scales on the right. The parameters displayed below are the time in UT, the geographic latitude and longitude, and the geomagnetic latitude. As usual for a low-altitude satellite, there is a cutoff frequency (~350 Hz) close to the proton gyrofrequency (see text).

modulation observed by the same satellite. DEMETER was a microsatellite in operation between June 2004 and December 2010. Its orbit was circular (660 km), polar, and nearly Sun-synchronous (10.30 LT and 22.30 LT). Its payload measured electromagnetic waves in different frequency ranges from ULF to MF and also plasma parameters (for example, the ion density and composition were given by the IAP experiment). The description of the experiments and of the raw data processing can be found in *Parrot* [2006]. The electric and magnetic spectrograms were always onboard calculated with a low time (2 s) and frequency (19 Hz) resolution, but the wave experiment was sometimes in a burst mode (waveforms are registered) which allows a spectral analysis with a much better resolution. Examples of EN emissions with QP modulation are shown in section 2, as well as some statistical results. Detailed analyses and discussion are done in section 3, whereas section 4 presents conclusions.

2. The Events

During the lifetime of DEMETER a total of 103 EN events with QP modulation have been recorded. Among these 103 events only 24 are recorded during a burst mode, and a detailed analysis will be done for three of them. Figure 1 presents electric and magnetic data recorded close to the magnetic equator on 10 November 2004 in daytime. The period corresponds to the recovery phase of an important magnetic storm. The minimum value of the *Dst* index was equal to −374 nT on 8 November 2004 at 07:00:00 UT and −122 nT at the time of the record. Another example recorded after the same magnetic storm is displayed in *Berthelier et al*. [2006, Figure 7]. These spectrograms present a funnel-shaped structure which is similar to observations performed by *Boardsen et al*. [1992] in the equatorial region at higher L values although the generation mechanism could be different. In Figure 1 the two vertical white lines bound the time interval when the wave experiment was in burst mode, and a more detailed spectral analysis is then presented in Figure 2. One can see QP emissions where each element contains horizontal line emissions both on the electric and the magnetic spectrograms. The satellite crosses the magnetic equator at 20:38:00 UT. In the magnetic spectrogram the lines above 1 kHz are due to onboard interferences. Another example of EN emissions with QP modulation is given in Figure 3 which corresponds to data recorded on 16 May 2005 between 15:42:00 UT and 15:45:00 UT in daytime. Once again this event was recorded during the recovery phase of a magnetic storm. The minimum value of the *Dst* index was equal to −247 nT on 15 May 2005 at 09:00:00 UT and −81 nT at the

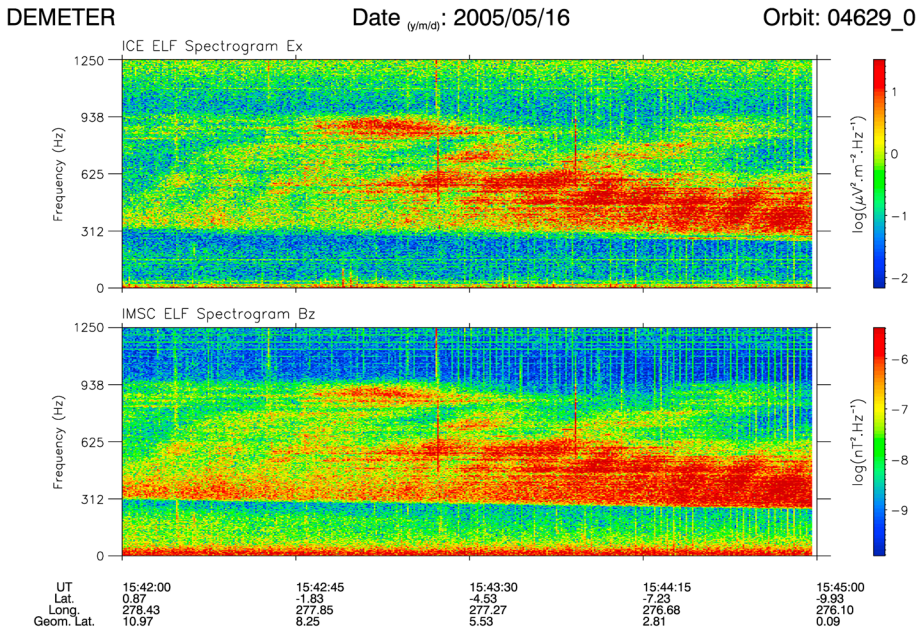

Figure 3. Same as Figure 2 but for data recorded on 16 May 2005 between 15:42:00 UT and 15:45:00 UT.

time of the record. A last example recorded on 13 September 2005 between 14:56:30 UT and 14:59:00 UT in daytime is shown in Figure 4. For this event, the minimum value of the *Dst* index was equal to −139 nT on 11 September 2005 at 11:00:00 UT and −79 nT at the time of the record.

In all spectrograms there is a cutoff frequency at $f_{L=0}$ (~350 Hz in Figure 2) which is close to the local proton gyrofrequency f_{cp} [*Santolík and Parrot*, 1999]. A comparison between $f_{L=0}$ and f_{cp} using equation (1) of *Santolík et al*. [2016] gives an estimation of the relative O^+ composition. For example, in Figure 3 at 15:42:00 UT one can see that $f_{L=0} = 312$ Hz and at the same time a magnetic field model indicates that $f_{cp} = 341$ Hz. This gives 91% of O^+ ions. The IAP experiment also confirmed that the ions O+ are by far the majority during our three events (not shown).

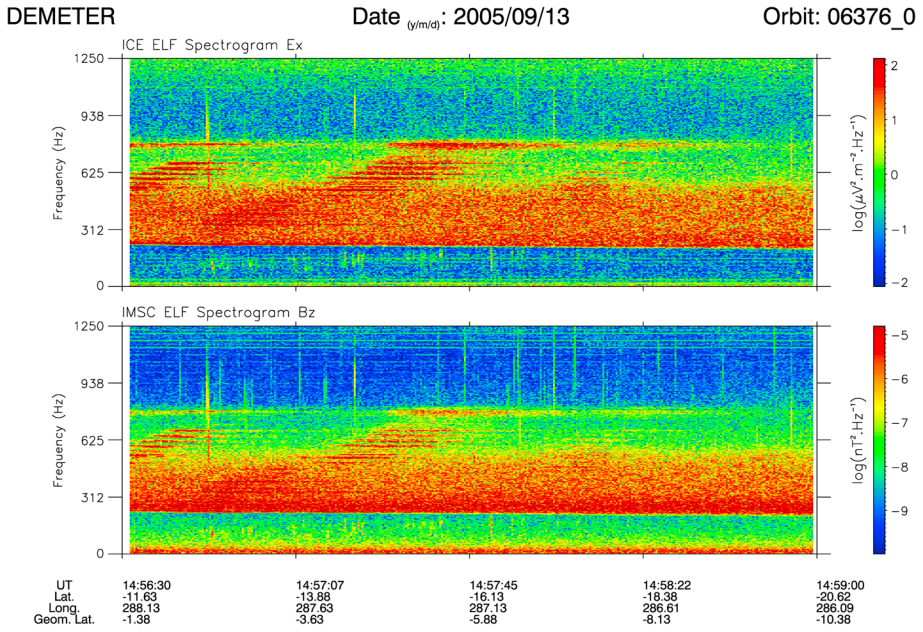

Figure 4. Same as Figure 2 but for data recorded on 13 September 2005 between 14:56:30 UT and 14:59:00 UT.

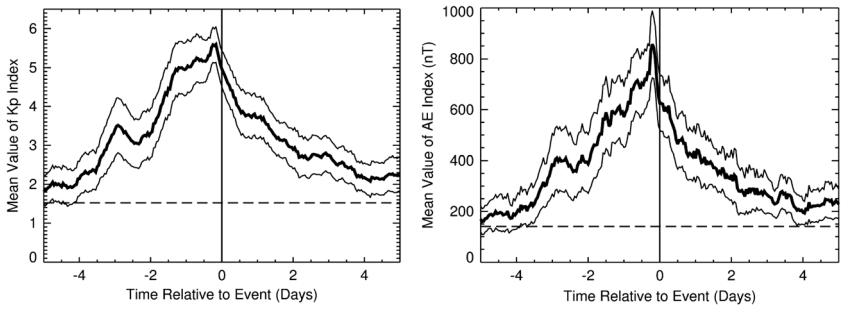

Figure 5. (left) Mean value of the *Kp* index as a function of the time relative to the 103 equatorial QP events shown by the bold line. The corresponding $\pm 3\sigma$ interval is represented by the two thin lines. (right) The same as on the left but for the *AE* index.

The 103 events are mainly dayside, but there are some events during nighttime (10) which are recorded during very large magnetic storms. Figure 5 presents the results of a superposed epoch analysis to check the mean values of the *Kp* and *AE* indexes at the time of the 103 events. It can be compared with Figure 2 of *Hayosh et al*. [2014] obtained with the same method (1 h time bins spanning from −5 days to +5 days after the time of the events) but for QP events recorded at various latitudes. One can see, first, that our equatorial events occur shortly (a few hours) after the maximum intensity of a magnetic storm, and second that the magnetic activity at the time of their registrations is much larger than the magnetic activity at the time of the QP events reported by *Hayosh et al*. [2014] at all latitudes. A similar analysis has been also done with the *Dst* index (not shown), and it indicates that *Dst* must be in average equal to −90 nT.

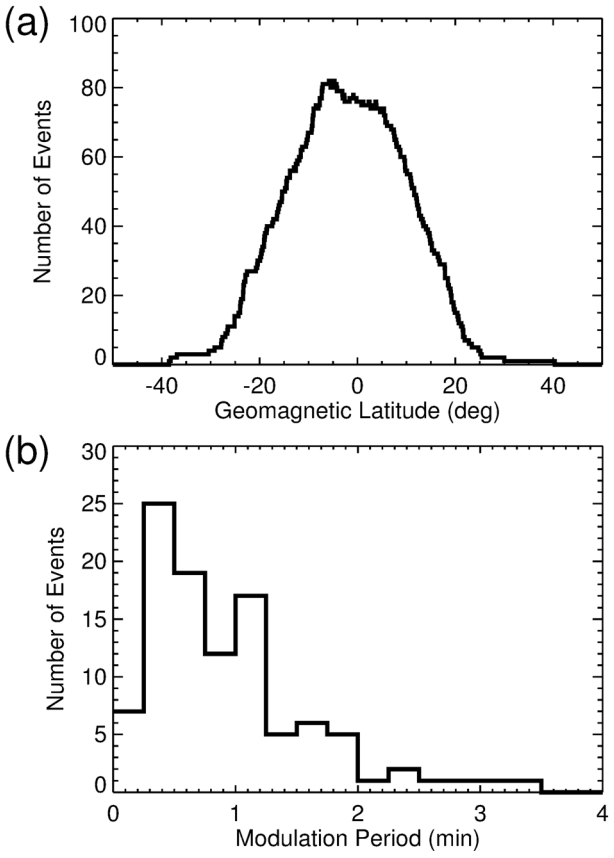

Figure 6. (a) Histogram of the number of events as a function of the geomagnetic latitude which is not normalized because the total latitudinal lengths of each of the 103 events have been considered. (b) Histogram of the number of events as a function of the modulation period which was determined as the median of time separations between consecutive QP elements of each event.

The histogram shown in Figure 6a indicates that the EN emissions are well located around the magnetic equator, but they can extend up to 20° in geomagnetic latitude. The histogram shown in Figure 6b indicates that the modulation periods of the QP elements are usually around 30 s and can be as large as 2 min. This period is a little bit lower than the Cluster period of the EN QP elements observed by *Němec et al*. [2015b] which spread from 30 s up to 4 min with a peak between 1 and 2 min. However, the authors note that they might have missed events with short modulation periods during their identification.

When there is no burst mode it is difficult to say if there is a line structure inside each QP element. But for the 24 events recorded during a burst mode this line structure is always present. It is problematical to determine specific harmonics in these line structures because the emissions can come from different

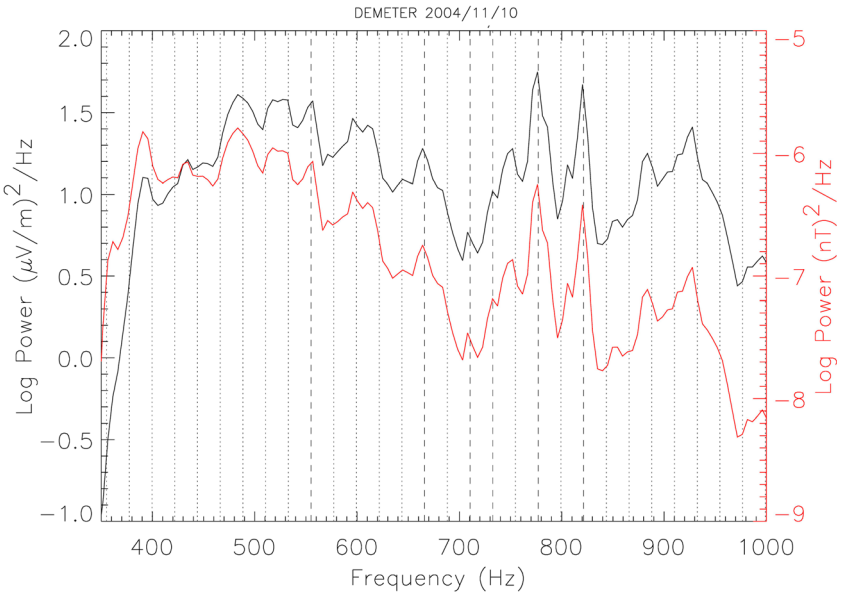

Figure 7. Spectra of the electric (black curve, left axis) and magnetic (red curve, right axis) fields recorded on 10 November 2004 in the ELF range between 350 and 1000 Hz (see Figure 2). The spectral analysis was done with the following parameters: 512 points fast Fourier transform (FFT), 20% overlapping, and a Blackman-Harris window. It corresponds to the average of 379 individual spectra between 20:38:15 UT and 20:39:15 UT. The vertical dotted and dashed lines are located at multiples of 22.2 Hz. The lines are dashed when there is a good fit with spectral peaks.

radial distances and then produce a mixture of lines with very different frequencies, but it was possible for the three selected events presented above to isolate a parent frequency, and they are analyzed in more detail in the next section.

3. Analyses and Discussion

A careful spectral analysis of the events shown in Figures 2–4 has been done in order to identify the frequency of the lines present in the QP elements. In this process the more intense spectral lines were first selected and then used to find a set of harmonics. It appears that most of these lines are at high harmonics of a parent frequency. The detailed spectral analysis of the electric and the magnetic fields for the 10 November 2004 event (Figure 2) is shown in Figure 7. One can observe frequencies of lines at multiple of 22.2 Hz, a frequency which is close to the local gyrofrequency f_{cO+} of the ion O^+ because during the time interval of Figure 2 the local proton gyrofrequency f_{cH+} (calculated with a magnetic field model) varies from 358.4 Hz to 374.4 Hz, i.e., f_{cO+} varies from 22.4 Hz to 23.4 Hz. On 16 May 2005 (Figure 3), some frequencies of lines are seen at multiple of 17 Hz whereas the local value of f_{cO+} varies from 21.3 Hz to 19.0 Hz during the time interval of Figure 3. This means that 17 Hz corresponds to a gyrofrequency f_{cO+} slightly above the satellite (Using a magnetic field model, one can calculate that 17 Hz corresponds to an altitude of ~ 1000 km.). The detailed spectral analysis of the electric and the magnetic fields for this event is shown in Figure 8. It reveals that several spectral components at high harmonics of 17 Hz can be detected between 400 and 600 Hz and also around 800 Hz with a lower intensity. They are at the same frequencies on the electric and on the magnetic spectra. In the same manner, on 13 September 2005 (Figure 9), some frequencies of lines are multiples of 13.7 Hz whereas the local value of f_{cO+} varies from 17.9 Hz to 17.5 Hz during the time interval of Figure 4. This parent frequency of 13.7 Hz corresponds to a gyrofrequency f_{cO+} at 600 km above the satellite.

When the acquisition system is in burst mode, the waveforms of the six components of the electromagnetic field are available up to 1.25 kHz, and it is possible to determine the propagation characteristics of the waves. The wave analysis is done in a coordinate system linked to the local magnetic field B_0 where the z axis is oriented along B_0, the x axis—which is in the local meridian plane—points toward larger L values, and the y axis completes the orthogonal system. This analysis is presented in Figure 10 which corresponds to the data shown in Figure 2 (10 November 2004). Frequency-time spectrograms of the electric and magnetic field

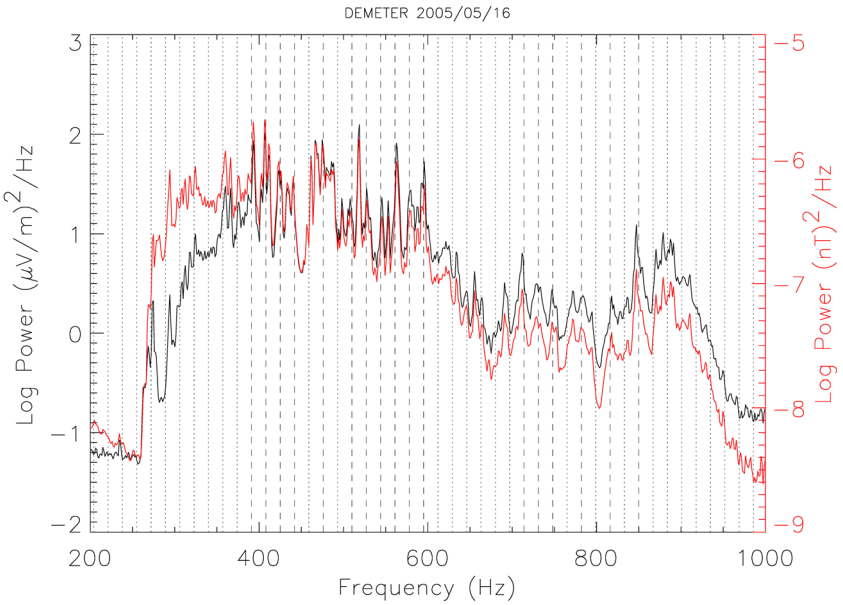

Figure 8. Spectra of the electric (black curve, left axis) and magnetic (red curve, right axis) fields recorded on 16 May 2005 in the ELF range between 200 and 1000 Hz (see Figure 3). The spectral analysis was done with the following parameters: 2048 points FFT, 10% overlapping, and a Blackman-Harris window. It corresponds to the average of 182 individual spectra between 15:42:45 UT and 15:45:00 UT. The vertical dotted and dashed lines are located at multiples of 17 Hz. The lines are dashed when there is a good fit with spectral peaks.

fluctuations are shown in Figures 10a and 10b, respectively. Figures 10c and 10d display the ellipticity of the magnetic and electric field fluctuations, respectively. The values of ellipticity varies from 0 (linear polarization) to 1 (circular polarization). Figure 10e shows the wave normal angle θ defined as the angle between B_0 and the wave vector **k**, whereas Figure 10f is related to the azimuthal angle ϕ measured from the *x* axis. These two angles are estimated by the electromagnetic singular value decomposition method [*Santolík et al.*, 2003].

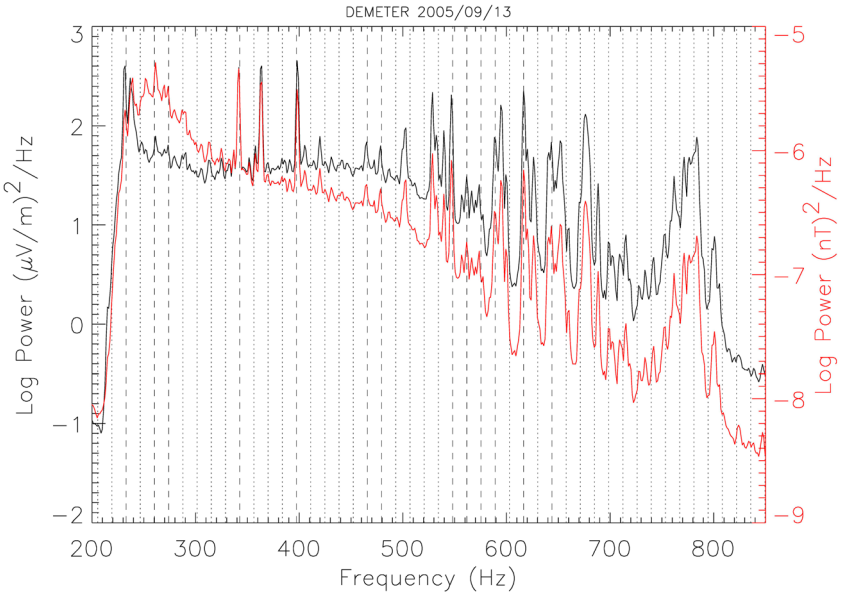

Figure 9. Spectra of the electric (black curve, left axis) and magnetic (red curve, right axis) fields recorded on 13 September 2005 in the ELF range between 200 and 850 Hz (see Figure 4). The spectral analysis was done with the following parameters: 2048 points FFT, 10% overlapping, and a Blackman-Harris window. It corresponds to the average of 162 individual spectra between 14:56:30 UT and 14:58:30 UT. The vertical dotted and dashed lines are located at multiples of 13.7 Hz. The lines are dashed when there is a good fit with spectral peaks.

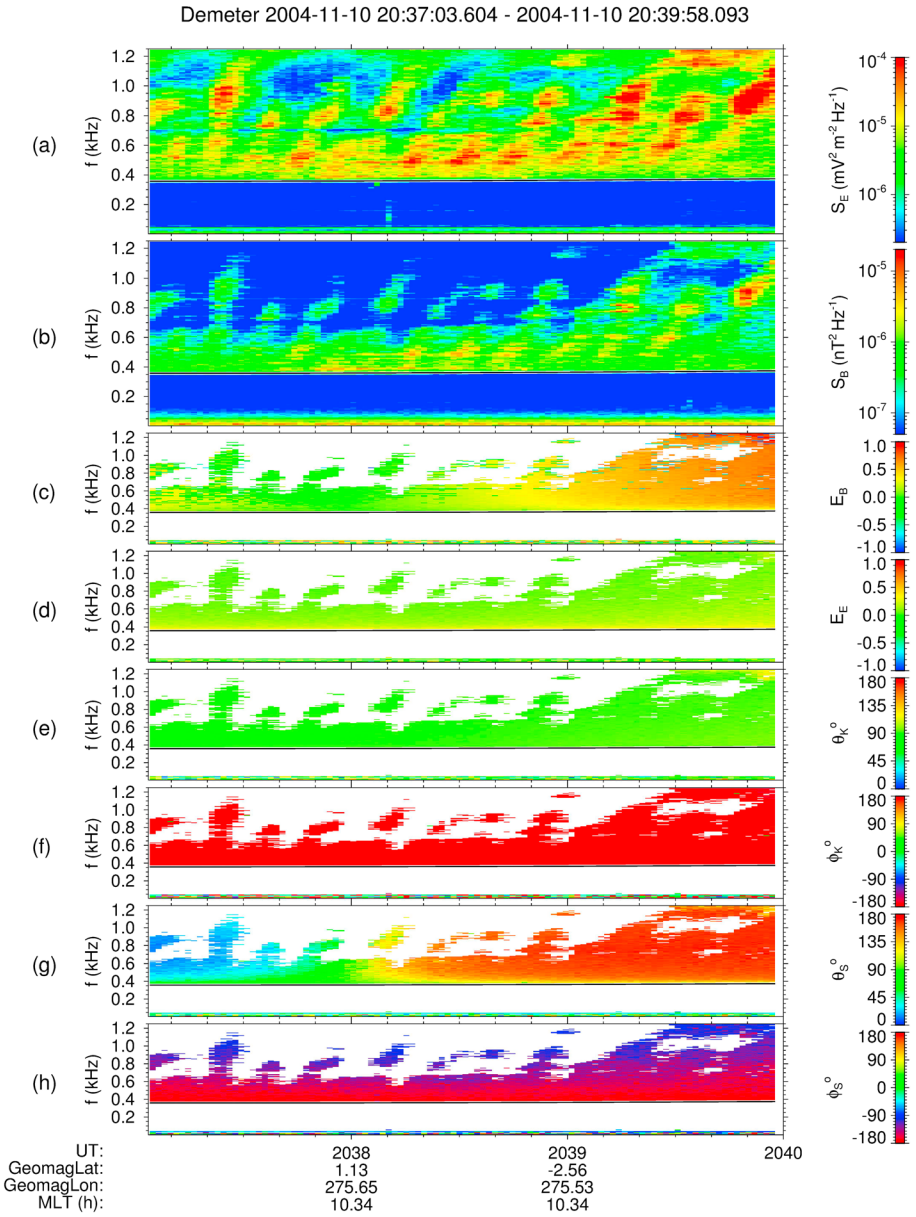

Figure 10. Wave propagation analysis of the data shown in Figure 2. (a) The sum of the three electric spectra; (b) the sum of the three magnetic spectra; (c) the ellipticity of the magnetic field fluctuations; (d) the ellipticity of the electric field fluctuations; (e and f) the wave normal angles θ and ϕ, respectively; and (g and h) the direction of the Poynting vector (see text for explanation). In each panel the black line indicates the proton gyrofrequency which varies from 358.4 Hz to 374.4 Hz. The empty areas in Figures 10c–10h correspond to frequency-time intervals with magnetic power spectral densities below 10^{-7} nT^2 Hz^{-1} or electric power spectral densities below 10^{-6} mV^2 m^{-2} Hz^{-1}. These areas are empty because the analysis is not meaningful for low-power waves. The UT, the geomagnetic latitude and longitude, and the magnetic local time are indicated below.

Figures 10g and 10h give the polar and the azimuthal angles which define the Poynting vector direction in the same frame of reference as before [*Santolík et al.*, 2001]. The results of this multidimensional analysis as functions of UT and frequency indicate the following.

1. When DEMETER is close to the equator, the value of the ellipticity is close to 0 which corresponds to a linear polarization of the magnetic field fluctuations.
2. The waves propagate with the **k** vector quasi-perpendicular (θ values close to 90°) as it was already underlined by *Hayosh et al.* [2016].

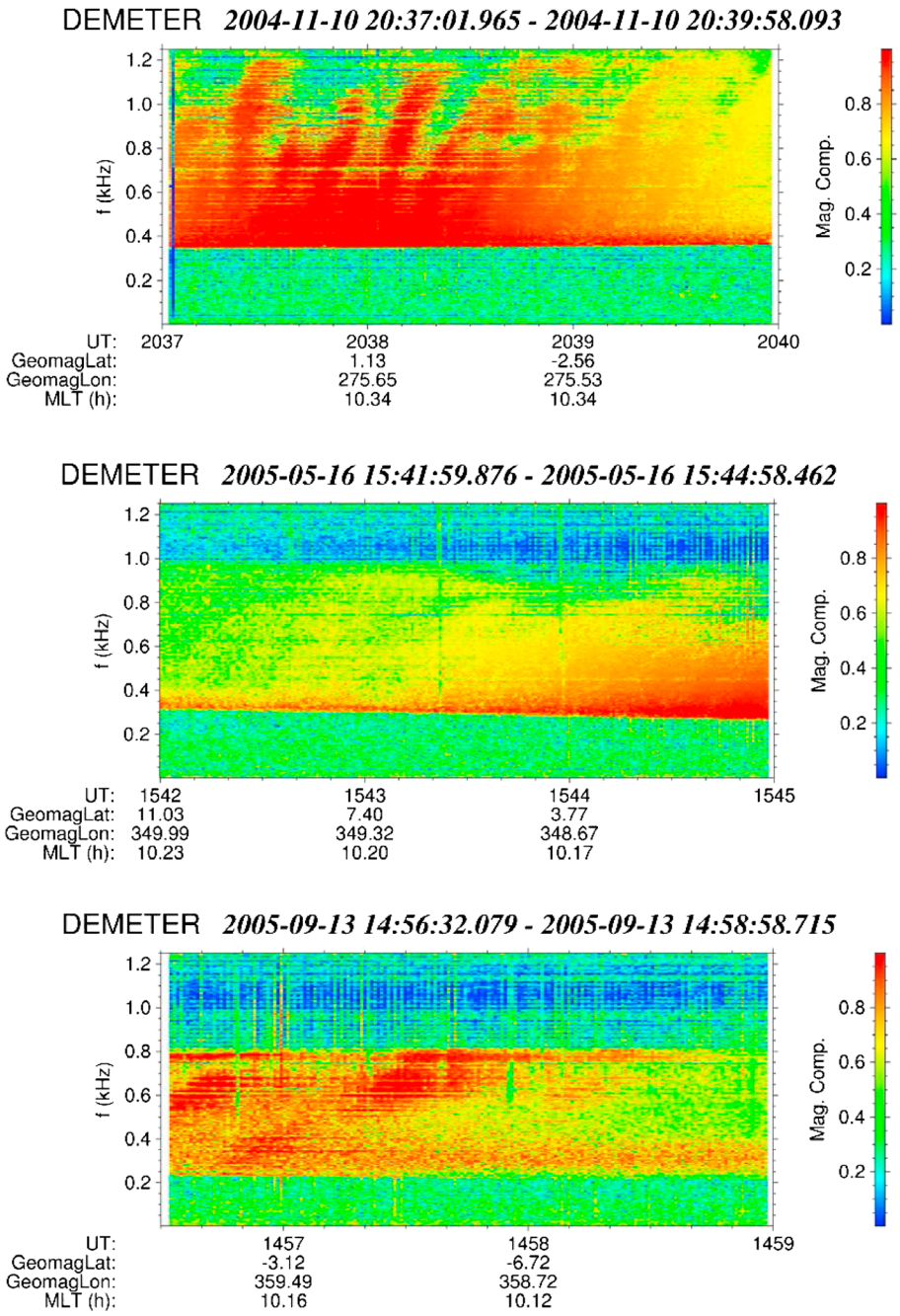

Figure 11. Spectrograms of the magnetic compressibility (see text for explanation) calculated for the three events presented in this paper. (top, middle, and bottom) Images correspond to Figures 2–4. The values of the magnetic compressibility are color coded according to the right scales.

3. The waves propagate with the azimuthal angle of the **k** vector close to 180° indicating that they are coming from above the satellite.

The two first points are expected for EN waves [e.g., *Santolík et al.*, 2004; *Meredith et al.*, 2008; *Němec et al.*, 2015b], and the third point is consistent with a source of the emission above the spacecraft (S/C). The mode of our events has been additionally identified by calculating the magnetic compressibility because the EN is characterized by a high magnetic compressibility [*Boardsen et al.*, 2016]. This parameter which has been evaluated as the ratio of parallel over total power spectral density of the magnetic field is shown in Figure 11 for

the three events previously selected. One can see that the magnetic compressibility is larger than 0.8 for the waves observed during these three events.

Concerning the direction of the Poynting vector, it is observed that the azimuthal angle is rather constant (~180°) whereas the value of the polar angle is equal to 90° at the magnetic equator. At larger geomagnetic latitudes the Poynting vector diverges away from the geomagnetic equator. The analysis of this effect is beyond the scope of the presend paper and will be analyzed in the future. Nevertheless, the observed propagation properties of the EN waves demonstrate that the source of these emissions with QP elements is in the ionosphere at the equator and slightly above the altitude of the satellite.

This is the first time that such observations of EN elements at multiples of the gyrofrequency f_{cO+} of the ion O^+ are done in the equatorial ionosphere because normally the EN elements are observed at multiples of the proton gyrofrequency [see, e.g., *Balikhin et al*., 2015] at much higher altitudes. To explain our observations, another possibility which could be considered is that, first, our EN elements are generated at the harmonics of the proton gyrofrequency at larger distances (higher L values) and, second, they propagated down in the ionosphere. But it is difficult to believe that by chance, for our three events, the multiples of the gyrofrequency f_{cO+} close to the location of observations exactly match the multiples of the proton gyrofrequency measured at the higher altitudes where a possible generation of these events could occur.

In the past such equatorial emissions at the harmonics of the O^+ ion gyrofrequency have been detected by *Liu et al*. [1994] during magnetic storms using AKEBONO data. The main differences are that they are located at $L = 1.5–2.5$ and that the harmonic order of the O^+ gyrofrequency is less than 10, whereas it is larger than 20 for the DEMETER events. According to the observations of *Liu et al*. [1994], the generation of waves in the presence of O^+ ions of ionospheric origin has been theoretically studied by *Pokhotelov et al*. [1997].

These emissions are observed on several consecutive half-orbits. For example, on 13 September 2005 (Figure 4), the EN waves with QP modulation are observed by DEMETER during five consecutive half-orbits, i.e., from a longitude of 340°E up to a longitude of 240°E. The corresponding time interval is between 11:39:00 UT and 18:12:00 UT. It means that the equatorial emissions cover more than 100° in longitude during 7.5 h. At the same time period there are four Cluster satellites at much higher altitudes in the magnetosphere. On board these satellites, the measurements of electromagnetic waves were performed by the Spatio Temporal Analysis of Field Fluctuations (STAFF) instrument [*Cornilleau-Wehrlin et al*., 1997, 2003]. Figure 12 shows four frequency-time spectrograms of the magnetic field recorded on 13 September 2005 which correspond to the data recorded by the four satellites (see also *Walker et al*. [2015b] who studied the same event). One can see an emission around 100 Hz when the satellites successively cross the magnetic equator. It occurs at 17:10:00 UT, 18:03:00 UT, 20:25:00 UT, and 20:38:00 UT for C2, C1, C3, and C4, respectively. This time interval corresponds to a longitudinal interval of 51° (between 277°E for C2 and 226°E for C4) which is inside the equatorial circular sector of the DEMETER observations. The relative positions of the Cluster S/C and DEMETER in the magnetic equatorial plane are shown in Figure 13 as a function of time. These Cluster equatorial emissions have been fully described by *Hrbáčková et al*. [2015] and *Němec et al*. [2015a, 2015b]. Fortunately, the wave experiment is in burst mode around 18:03:00 UT when C1 crosses the equator, and Figure 14 presents a detailed spectrogram of the magnetic field between 18:00:00 UT and 18:10:00 UT. This spectrogram shows a similar pattern as DEMETER has observed, i.e., QP elements with line structures, but the lines are at much lower frequencies. These Cluster equatorial QP emissions have been discussed by *Němec et al*. [2015b]. Concerning our event, the frequency interval between the lines is of the order of 3.1 Hz which is the mean value of the local proton gyrofrequency as from the measured magnetic field in the time interval 18:00–18:10 UT.

These emissions are identical to the EN waves at the multiple of the proton gyrofrequency observed with Cluster by *Balikhin et al*. [2015] who have demonstrated that they are generated by unstable ion ring distributions. Using also Cluster data, *Santolík et al*. [2002] have noticed that the emission lines may be not exactly at harmonics of the local proton gyrofrequency. They suggested that the waves could be generated at other locations (near the equator) and that they can propagate to the area of observation. For our observation this means that, C1 being at 4.93 R_E, the source must be at 5.29 R_E.

For this event, the QP period is different on DEMETER (~45 s) and on Cluster (~105 s). This is consistent with the average values of the statistical results shown in Figure 6b for DEMETER and reported by *Němec et al*. [2015b] for Cluster (see section 2). It is also noticed that the observed QP modulation is a constant effect

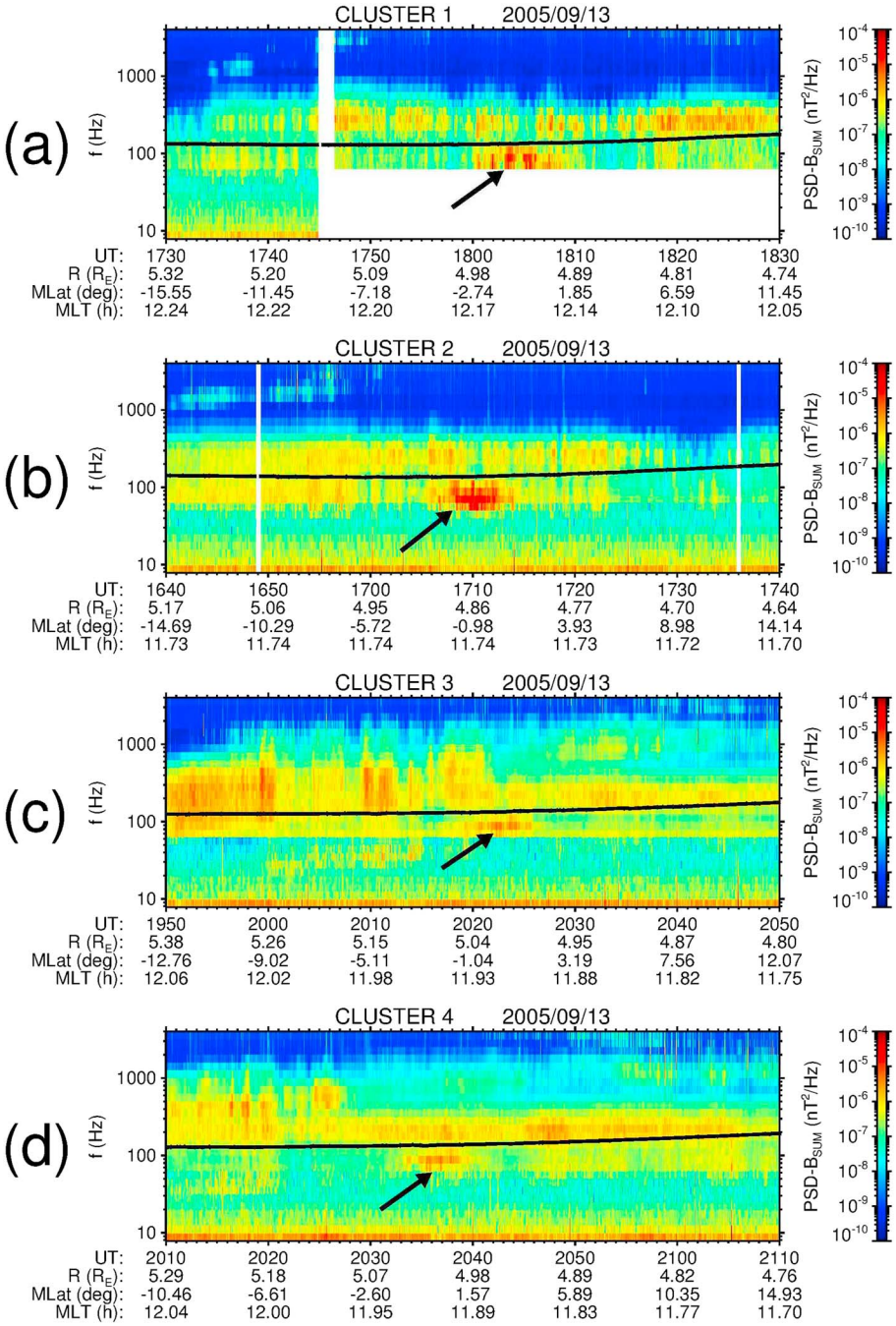

Figure 12. Magnetic field spectrograms recorded by the four Cluster satellites on 13 September 2005 when they cross the magnetic equator. (a–d) Images correspond to C1, C2, C3, and C4. The plots are done with the STAFF-SA data of which the frequency range is logarithmic between 8 Hz and 4 kHz. For each satellite, the lower hybrid frequency is plotted with a black line. The orbital information (radial distance, magnetic latitude, and magnetic local time) is indicated for each S/C. The intensities of the spectrograms are color coded according to the scales on the right. In each panel, the arrow indicates the position of the EN noise (at frequencies around 100 Hz) when the S/C crosses the magnetic equator.

whatever is the location of the waves in the equatorial plane, in the ionosphere, or at larger radial distances as it was already underlined by *Němec et al*. [2013a]. The QP modulation mechanism has been investigated by *Němec et al*. [2015b]. They attribute this observed QP modulation of EN wave intensity to compressional magnetic field pulsations. *Němec et al*. [2013a, 2016] also discussed the fact that the periods of simultaneous QP emissions are sometimes not equal at different distances.

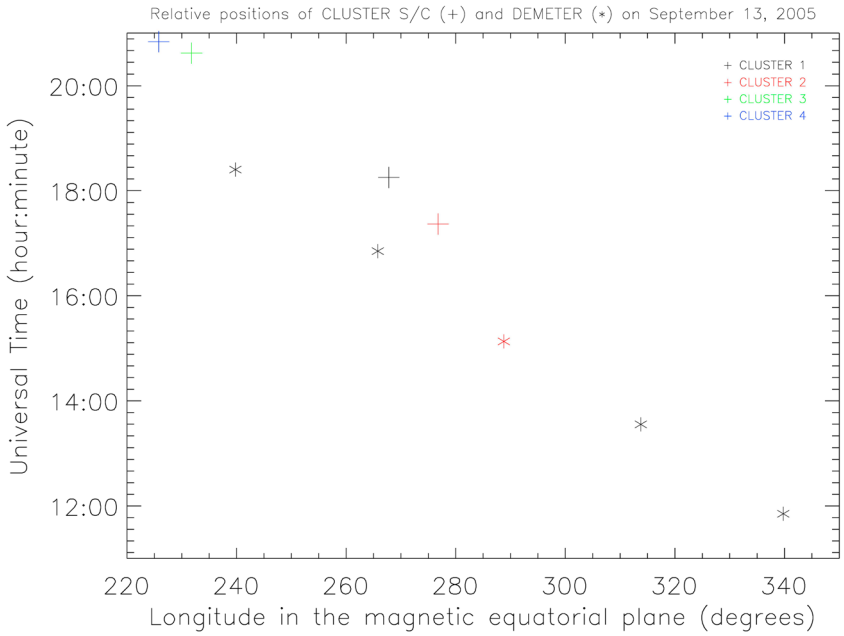

Figure 13. Geocentric longitudes and times of the four Cluster spacecraft and DEMETER when they cross the magnetic equator on 13 September 2005. The positions of the Cluster S/C are indicated by a cross which is color coded according to the insert in the right top corner. The data related to C1 are shown in Figure 14. The positions of DEMETER are indicated by a star, and they correspond to the crossing of the magnetic equator for five consecutive orbits. The data related to the red star are shown in Figure 4. The displayed time interval corresponds to observations of EN by all spacecraft. In this magnetic equatorial plane the four Cluster S/C are at a radial distance of ~5 R_E, whereas DEMETER is at ~1.1 R_E.

4. Conclusions

EN emissions with QP modulation observed on board the low-altitude satellite DEMETER have been studied. The results indicate the following.

1. They occur just after very large magnetic storms when, in average, $Kp = 5$, $AE = 800$ nT, and $Dst = -90$ nT.

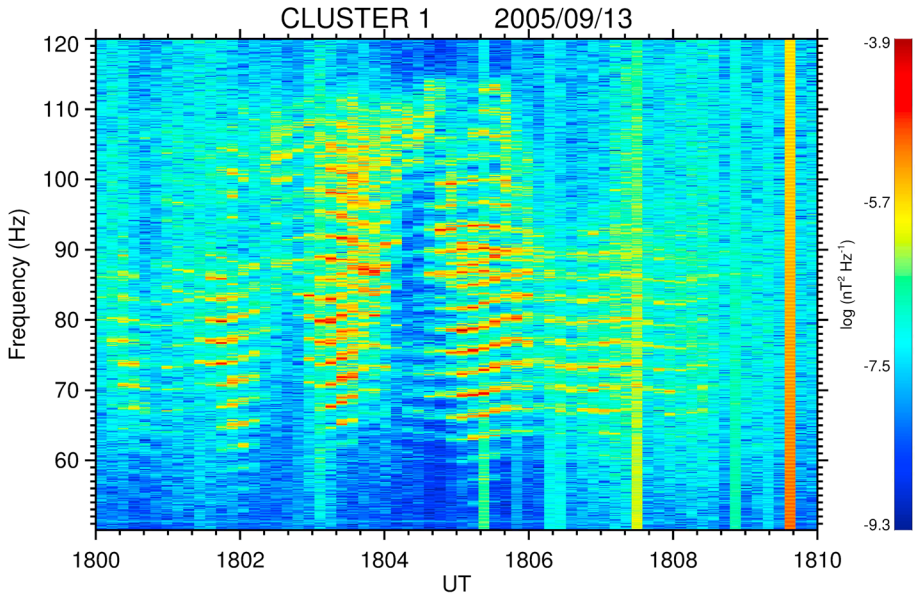

Figure 14. Zoom of the magnetic field spectrogram recorded by C1 between 18:00:00 UT and 18:10:00 UT (see Figure 12a). The plot uses high-resolution STAFF-SC data available during the burst mode. The frequency range is from 50 to 120 Hz. The intensity of the spectrogram is color coded according to the scale on the right. It has been evaluated that the frequency spacing between the lines is of the order of 3.1 Hz.

2. Their spectrograms often present a funnel-shaped structure which will be studied in a future work.
3. They can be observed during several hours in large equatorial areas.
4. The detailed analysis of a selection of three events has shown that this EN with QP emissions propagates with a wave normal angle close to 90°, an ellipticity close to 0, and a high magnetic compressibility.
5. Thanks to a simultaneous observation with DEMETER and Cluster, it has been shown that a QP modulation exists simultaneously in the equatorial plane in the ionosphere and at much higher altitudes although their periods are different.
6. For the first time, it has been shown that the EN emissions observed in the ionosphere have structures linked to a gyrofrequency of the ion O^+ estimated at a location close or just above the satellite.

Finally, these EN noise with QP modulation could be related to waves with rising-tone features in their spectrogram recently observed by *Fu et al*. [2014] and *Boardsen et al*. [2014].

Acknowledgments
This work is mainly related to data recorded by the electric field experiment ICE and the magnetic field experiment IMSC of the microsatellite DEMETER which was operated by the French Centre National d'Etudes Spatiales (CNES). The authors thank the PI of ICE and IAP (J.J. Berthelier) for the use of the data. The DEMETER data shown in this paper can be obtained at https://cdpp-archive.cnes.fr/, whereas the Cluster data are available at http://www.cosmos.esa.int/web/csa. The work of F.N. was supported by GACR grant 15-01775Y. O.S. was supported by GACR grant 14-31899S, MSMT grant LH15304, and by the Praemium Academiae Award.

References

Balikhin, M. A., Y. Y. Shprits, S. N. Walker, L. Chen, N. Cornilleau-Wehrlin, I. Dandouras, O. Santolik, C. Carr, K. H. Yearby, and B. Weiss (2015), Observations of discrete harmonics emerging from equatorial noise, *Nat. Commun.*, *6*, 7703, doi:10.1038/ncomms8703.

Berthelier, J. J., et al. (2006), ICE, the electric field experiment on DEMETER, *Planet. Space Sci.*, *54*(5), 456–471, doi:10.1016/j.pss.2005.10.016.

Boardsen, S. A., D. L. Gallagher, D. A. Gurnett, W. K. Peterson, and J. L. Green (1992), Funnel-shaped, low-frequency equatorial waves, *J. Geophys. Res.*, *97*, 14,967–14,976, doi:10.1029/92JA00827.

Boardsen, S. A., G. B. Hospodarsky, C. A. Kletzing, R. F. Pfaff, W. S. Kurth, J. R. Wygant, and E. A. MacDonald (2014), Van Allen Probe observations of periodic rising frequencies of the fast magnetosonic mode, *Geophys. Res. Lett.*, *41*, 8161–8168, doi:10.1002/2014GL062020.

Boardsen, S. A., et al. (2016), Survey of the frequency dependent latitudinal distribution of the fast magnetosonic wave mode from Van Allen Probes electric and magnetic field instrument and integrated science waveform receiver plasma wave analysis, *J. Geophys. Res. Space Physics*, *121*, 2902–2921, doi:10.1002/2015JA021844.

Bortnik, J., and R. M. Thorne (2010), Transit time scattering of energetic electrons due to equatorially confined magnetosonic waves, *J. Geophys. Res.*, *115*, A07213, doi:10.1029/2010JA015283.

Chen, L., and R. M. Thorne (2012), Perpendicular propagation of magnetosonic waves, *Geophys. Res. Lett.*, *39*, L14102, doi:10.1029/2012GL052485.

Chen, L., R. M. Thorne, V. K. Jordanova, and R. B. Horne (2010), Global simulation of magnetosonic wave instability in the storm time magnetosphere, *J. Geophys. Res.*, *115*, A11222, doi:10.1029/2010JA015707.

Chen, L., R. M. Thorne, V. K. Jordanova, M. F. Thomsen, and R. B. Horne (2011), Magnetosonic wave instability analysis for proton ring distributions observed by the LANL magnetospheric plasma analyzer, *J. Geophys. Res.*, *116*, A03223, doi:10.1029/2010JA016068.

Cornilleau-Wehrlin, N., et al. (1997), The Cluster Spatio-Temporal Analysis of Field Fluctuations (STAFF) experiment, *Space Sci. Rev.*, *79*, 107–136, doi:10.1023/A:1004979209565.

Cornilleau-Wehrlin, N., et al. (2003), First results obtained by the Cluster STAFF experiment, *Ann. Geophys.*, *21*, 437–456, doi:10.5194/angeo-21-437-2003.

Fu, H. S., J. B. Cao, Z. Zhima, Y. V. Khotyaintsev, V. Angelopoulos, O. Santolík, Y. Omura, U. Taubenschuss, L. Chen, and S. Y. Huang (2014), First observation of rising-tone magnetosonic waves, *Geophys. Res. Lett.*, *41*, 7419–7426, doi:10.1002/2014GL061867.

Gurnett, D. A. (1976), Plasma wave interactions with energetic ions near the magnetic equator, *J. Geophys. Res.*, *81*, 2765–2770, doi:10.1029/JA081i016p02765.

Hayosh, M., F. Němec, O. Santolík, and M. Parrot (2014), Statistical investigation of VLF quasi-periodic emissions measured by the DEMETER spacecraft, *J. Geophys. Res. Space Physics*, *119*, 8063–8072, doi:10.1002/2013JA019731.

Hayosh, M., F. Němec, O. Santolík, and M. Parrot (2016), Propagation properties of quasi-periodic emissions observed by the DEMETER spacecraft, *Geophys. Res. Lett.*, *43*, 1007–1014, doi:10.1002/2015GL067373.

Horne, R. B., G. V. Wheeler, and H. S. C. K. Alleyne (2000), Proton and electron heating by radially propagating fast magnetosonic waves, *J. Geophys. Res.*, *105*, 27,597–27,610, doi:10.1029/2000JA000018.

Horne, R. B., R. M. Thorne, S. A. Glauert, N. P. Meredith, D. Pokhotelov, and O. Santolík (2007), Electron acceleration in the Van Allen radiation belts by fast magnetosonic waves, *Geophys. Res. Lett.*, *34*, L17107, doi:10.1029/2007GL030267.

Hrbáčková, Z., O. Santolík, F. Němec, E. Macušova, and N. Cornilleau-Wehrlin (2015), Systematic analysis of occurrence of equatorial noise emissions using 10 years of data from the Cluster mission, *J. Geophys. Res. Space Physics*, *120*, 1007–1021, doi:10.1002/2014JA020268.

Kasahara, Y., H. Kenmochi, and I. Kimura (1994), Propagation characteristics of the ELF emissions observed by the satellite Akebono in the magnetic equatorial region, *Radio Sci.*, *29*, 751–767, doi:10.1029/94RS00445.

Liu, H., S. Kokubun, and K. Hayashi (1994), Equatorial electromagnetic emission with discrete spectra near harmonics of oxygen gyrofrequency during magnetic storm, *Geophys. Res. Lett.*, *21*, 225–228, doi:10.1029/93GL02836.

Ma, Q., W. Li, L. Chen, R. M. Thorne, C. A. Kletzing, W. S. Kurth, G. B. Hospodarsky, G. D. Reeves, M. G. Henderson, and H. E. Spence (2014), The trapping of equatorial magnetosonic waves in the Earth's outer plasmasphere, *Geophys. Res. Lett.*, *41*, 6307–6313, doi:10.1002/2014GL061414.

Meredith, N. P., R. B. Horne, and R. R. Anderson (2008), Survey of magnetosonic waves and proton ring distributions in the Earth's inner magnetosphere, *J. Geophys. Res.*, *113*, A06213, doi:10.1029/2007JA012975.

Němec, F., O. Santolík, M. Parrot, and J. J. Berthelier (2007), Comparison of magnetospheric line radiation and power line harmonic radiation: A systematic survey using the DEMETER spacecraft, *J. Geophys. Res.*, *112*, A04301, doi:10.1029/2006JA012134.

Němec, F., O. Santolík, M. Parrot, J. S. Pickett, M. Hayosh, and N. Cornilleau-Wehrlin (2013a), Conjugate observations of quasi-periodic emissions by Cluster and DEMETER spacecraft, *J. Geophys. Res. Space Physics*, *118*, 198–208, doi:10.1029/2012JA018380.

Němec, F., O. Santolík, J. S. Pickett, M. Parrot, and N. Cornilleau-Wehrlin (2013b), Quasi-periodic emissions observed by the Cluster spacecraft and their association with ULF magnetic pulsations, *J. Geophys. Res. Space Physics*, *118*, 4210–4220, doi:10.1002/jgra.50406.

Němec, F., O. Santolík, Z. Hrbáčková, and N. Cornilleau-Wehrlin (2015a), Intensities and spatiotemporal variability of equatorial noise emissions observed by the Cluster spacecraft, *J. Geophys. Res. Space Physics*, *120*, 1620–1632, doi:10.1002/2014JA020814.

Němec, F., O. Santolík, Z. Hrbáčková, J. S. Pickett, and N. Cornilleau-Wehrlin (2015b), Equatorial noise emissions with quasiperiodic modulation of wave intensity, *J. Geophys. Res. Space Physics*, *120*, 2649–2661, doi:10.1002/2014JA020816.

Němec, F., G. Hospodarsky, J. S. Pickett, O. Santolík, W. S. Kurth, and C. Kletzing (2016), Conjugate observations of quasiperiodic emissions by the Cluster, Van Allen Probes, and THEMIS spacecraft, *J. Geophys. Res. Space Physics*, *121*, 7647–7663, doi:10.1002/2016JA022774.

Parrot, M. (2006), First results of the DEMETER micro-satellite, *Planet. Space Sci.*, *54*(5), 411–558, doi:10.1016/j.pss.2005.10.012.

Perraut, S., A. Roux, P. Robert, R. Gendrin, J. A. Sauvaud, J. M. Bosqued, G. Kremzer, and A. Korth (1982), A systematic study of ULF waves above F_{H+} from GEOS 1 and 2 measurements and their relationships with proton ring distributions, *J. Geophys. Res.*, *87*, 6219–6236, doi:10.1029/JA087iA08p06219.

Pokhotelov, O. A., D. O. Pokhotelov, F. Z. Feygin, V. A. Gladychev, M. Parrot, K. Hayashi, J. Kangas, and K. Mursula (1997), Oxygen cyclotron harmonic waves in the deep plasmasphere during magnetic storms, *J. Geophys. Res.*, *102*, 77–83, doi:10.1029/96JA03067.

Posch, J. L., M. J. Engebretson, C. N. Olson, S. A. Thaller, A. W. Breneman, J. R. Wygant, S. A. Boardsen, C. A. Kletzing, C. W. Smith, and G. D. Reeves (2015), Low-harmonic magnetosonic waves observed by the Van Allen Probes, *J. Geophys. Res. Space Physics*, *120*, 6230–6257, doi:10.1002/2015JA021179.

Russell, C. T., R. E. Holzer, and E. J. Smith (1970), Ogo 3 observations of ELF noise in the magnetosphere. 2. The nature of the equatorial noise, *J. Geophys. Res.*, *75*, 755–768, doi:10.1029/JA075i004p00755.

Santolík, O., and M. Parrot (1999), Case studies on wave propagation and polarization of ELF emissions observed by Freja around the local proton gyro-frequency, *J. Geophys. Res.*, *104*, 2459–2475, doi:10.1029/1998JA900045.

Santolík, O., F. Lefeuvre, M. Parrot, and J. L. Rauch (2001), Complete wave-vector directions of electromagnetic emissions: Application to INTERBALL-2 measurements in the nightside auroral zone, *J. Geophys. Res.*, *106*, 13,191–13,201, doi:10.1029/2000JA000275.

Santolík, O., J. S. Pickett, D. A. Gurnett, M. Maksimovic, and N. Cornilleau-Wehrlin (2002), Spatiotemporal variability and propagation of equatorial noise observed by Cluster, *J. Geophys. Res.*, *107*(A12), 1495, doi:10.1029/2001JA009159.

Santolík, O., M. Parrot, and F. Lefeuvre (2003), Singular value decomposition methods for wave propagation analysis, *Radio Sci.*, *38*(1), 1010, doi:10.1029/2000RS002523.

Santolík, O., F. Němec, K. Gereová, E. Macúšová, Y. de Conchy, and N. Cornilleau-Wehrlin (2004), Systematic analysis of equatorial noise below the lower hybrid frequency, *Ann. Geophys.*, *22*, 2587–2595, doi:10.5194/angeo-22-2587-2004.

Santolík, O., M. Parrot, and F. Němec (2016), Propagation of equatorial noise to low altitudes: Decoupling from the magnetosonic mode, *Geophys. Res. Lett.*, *43*, 6694–6704, doi:10.1002/2016GL069582.

Tsurutani, B. T., B. J. Falkowski, J. S. Pickett, O. P. Verkhoglyadova, O. Santolik, and G. S. Lakhina (2014), Extremely intense ELF magnetosonic waves: A survey of polar observations, *J. Geophys. Res. Space Physics*, *119*, 964–977, doi:10.1002/2013JA019284.

Walker, S. N., M. A. Balikhin, D. R. Shklyar, K. H. Yearby, P. Canu, C. M. Carr, and I. Dandouras (2015a), Experimental determination of the dispersion relation of magnetosonic waves, *J. Geophys. Res. Space Physics*, *120*, 9632–9650, doi:10.1002/2015JA021746.

Walker, S. N., M. A. Balikhin, S. A. Boardsen, and D. G. Sibeck (2015b), Cluster observations of non time continuous magnetosonic waves, paper presented at AGU Fall meeting, San Francisco.